Dynamic continuum pedestrian flow model with memory effect

Yinhua Xia,* S. C. Wong,† and Chi-Wang Shu‡
Division of Applied Mathematics, Brown University, Providence, Rhode Island 02912, USA
and Department of Civil Engineering, The University of Hong Kong, Hong Kong, China
(Received 30 April 2009; published 23 June 2009)

In this paper, we develop a macroscopic model for pedestrian flow using the dynamic continuum modeling approach. We consider a two-dimensional walking facility that is represented as a continuum within which pedestrians can move freely in any direction. A pedestrian chooses a route based on his or her memory of the shortest path to the desired destination when the facility is empty and, at the same time, tries to avoid high densities. In this model, pedestrian flow is governed by a two-dimensional conservation law, and a general speed-flow-density relationship is considered. The model equation is solved numerically using the discontinuous Galerkin method, and a numerical example is employed to demonstrate both the model and the effectiveness of the numerical method.

DOI: 10.1103/PhysRevE.79.066113 PACS number(s): 89.40.−a, 45.70.Vn

I. INTRODUCTION

Many models of pedestrian traffic dynamics have been formulated recently [1,2]. These models can generally be classified into two categories: microscopic models and macroscopic models. The former include the cellular automaton model [3–6], the social force model [7–10], and the lattice-gas model [11–14], and are particularly well suited for use with small crowds. Macroscopic models, in contrast, focus on the overall behavior of pedestrian flows and are more applicable to investigations of extremely large crowds, especially when examining aspects of motion in which individual differences are less important [15].

The continuum approach is widely used in the macroscopic modeling of traffic flow problems. The continuum modeling of transportation systems for steady-state user equilibrium problems has been particularly well investigated [16–19]. A systematic framework for the dynamic macroscopic modeling of pedestrian flow problems was given in [20], but the user equilibrium concept was not explicitly considered. To address this issue, Hoogendoorn *et al.* developed a predictive user equilibrium model, in which pedestrians were assumed to have perfect information with which to make their route choice decisions over time [21–23]. This modeling approach is useful for representing a more strategic level of route choice decisions whereby pedestrians accumulate travel information from their daily experiences or from some other sources. However, in certain applications, pedestrians may not have predictive information when they make a route choice decision [24]. Instead, they may have to rely on instantaneous information and change their choice in a reactive manner when walking through a facility (see [25] for the difference between predictive and reactive dynamic user equilibrium principles). Huang *et al.* [26] recently revisited the dynamic macroscopic model of pedestrian flow [20] in the context of the reactive user equilibrium principle. In the model, pedestrians from a given location choose the path that minimizes the individual walking costs to their destination based on the instantaneous travel cost information available to them at the time of making the decision.

In this paper, we also use the dynamic continuum approach to model pedestrian flow macroscopically. In our model, pedestrian density is governed by a scalar two-dimensional conservation law. The direction of the flow is determined by the route choice strategy, and the magnitude of the flow is determined by the relationships among the macroscopic variables of pedestrian speed, density, and flow. The route choice strategy in our model is different from those used in the aforementioned models and is based on the hypothesis that pedestrians seek to minimize their estimated travel cost based on memory, but temper that behavior to avoid high densities. The predictive user equilibrium model [21–23] requires that pedestrians have perfect information over time for use in choosing their route, whereas the reactive user equilibrium model [26] requires that they have instantaneous global information about the entire domain based on which they choose an instantaneous route. The hypothesis, on which our model is based, in contrast, posits that pedestrians choose an instantaneous route based on both the information stored in their memory and local instantaneous information. This route choice strategy thus falls between the strategies of predictive and reactive route choice. The main advantages of this model are that it does not require that pedestrians anticipate changes in the operating conditions over time, especially when they are not familiar with the likely responses of a crowd, and allows for circumstances in which the quality of the instantaneous information may be degraded due to adverse environmental conditions such as bad weather, insufficient lighting, and smoky conditions during escape from a fire.

To solve our model numerically, we adopt the discontinuous Galerkin (DG) method that was employed in [27] to solve the reactive equilibrium pedestrian model [26]. We do not need to solve the Eikonal equation at each time step in the numerical procedure, and thus avoid the most time-consuming aspect of that procedure [27]. The DG method is a type of finite element method that uses discontinuous piecewise polynomials as the solution and the test space. The

*yxia@dam.brown.edu
†hhecwsc@hkucc.hku.hk
‡shu@dam.brown.edu

first DG method was introduced in 1973 by Reed and Hill [28] in their framework for a neutron transport problem that involved a time-independent linear hyperbolic equation. Cockburn *et al.* first developed the method for hyperbolic conservation laws in a series of papers [29–32] in which they established a framework of solving nonlinear time-dependent problems more easily. Their framework employs explicit, nonlinearly stable, high-order Runge-Kutta time discretizations [33] and DG discretization in space with exact or approximate Riemann solvers as the interface fluxes and total variation bounded (TVB) nonlinear limiters to derive the nonoscillatory properties of strong shocks. The DG method is well suited to complex geometries, as it allows them to be applied on unstructured grids. It can also handle nonconforming elements by allowing the grids to have hanging nodes. It is highly parallelizable, as the elements are discontinuous and the intercommunications are minimal. The DG method has found wide application in such diverse fields as aeroacoustics, electromagnetism, gas dynamics, granular flows, magnetohydrodynamics, meteorology, the modeling of shallow water, oceanography, oil recovery simulation, semiconductor device simulation, the transport of contaminants in porous media, turbomachinery, turbulent flows, viscoelastic flows, and weather forecasting, among many others. For a detailed description of this method, its implementation, and applications for conservation laws, we refer interested readers to [34–42].

The remainder of this paper is organized as follows. In Sec. II, we describe our model of pedestrian flows and discuss the well posedness of the linearized equation. In Sec. III, we present the numerical algorithm for the model. A numerical example is given in Sec. IV to demonstrate the model and the effectiveness of the numerical method. Finally, we make some concluding remarks in Sec. V.

II. MODEL FORMULATION

A. Model equations

We consider a two-dimensional walking facility that is represented as a continuum with a domain $\Omega \in \mathbb{R}^2$, inflow boundary Γ_i, outflow boundary Γ_o, and solid-wall boundary $\Gamma_w(\partial\Omega=\Gamma_i \cup \Gamma_o \cup \Gamma_w)$. In domain Ω, we define $\rho(\boldsymbol{x},t)$ as the pedestrian density and $u(\boldsymbol{x},t)$ as the pedestrian walking speed (we consider an isotropic case in which speed is a scalar quality). Let $\boldsymbol{f}(\boldsymbol{x},t)=(f_1(\boldsymbol{x},t),f_2(\boldsymbol{x},t))$ be the vector of the flow flux in the walking facility. By default, $\boldsymbol{f}(\boldsymbol{x},t)=0$ on Γ_w. We further define $c(\boldsymbol{x},\rho(\boldsymbol{x},t))$ as the local cost per unit distance of movement at time t, which depends on the instantaneous pedestrian density and location $\boldsymbol{x}$.

Similar to many physical systems, pedestrian flow is governed by a conservation law,

$$\rho_t(\boldsymbol{x},t) + \nabla \cdot \boldsymbol{f}(\boldsymbol{x},t) = 0, \quad \forall\, \boldsymbol{x} \in \Omega, \tag{1}$$

where $\boldsymbol{x}=(x,y)$, $\rho_t(\boldsymbol{x},t)=\partial\rho(\boldsymbol{x},t)/\partial t$, and $\nabla\cdot\boldsymbol{f}(\boldsymbol{x},t) = \partial f_1(\boldsymbol{x},t)/\partial x + \partial f_2(\boldsymbol{x},t)/\partial y$.

We need to know the flow flux $\boldsymbol{f}(\boldsymbol{x},t)$ to establish the model, which comprises the magnitude and direction of this flux. To determine the magnitude of flux $\boldsymbol{f}(\boldsymbol{x},t)$, we need to know the relationships among the macroscopic variables of pedestrian speed, density, and flow. We assume that the pedestrian speed $u(\boldsymbol{x},t)$ depends on the pedestrian density,

$$u(\boldsymbol{x},t) = U(\boldsymbol{x},\rho(\boldsymbol{x},t)), \tag{2}$$

where $U(\boldsymbol{x},\rho)$ is the function of the pedestrian speed with respect to the density and location dependence. The flow intensity is then equal to the product of the pedestrian speed and density, that is,

$$\|\boldsymbol{f}(\boldsymbol{x},t)\| = \sqrt{f_1(\boldsymbol{x},t)^2 + f_2(\boldsymbol{x},t)^2} = u(\boldsymbol{x},t)\rho(\boldsymbol{x},t). \tag{3}$$

To determine the direction of the flow flux, it is necessary to formulate a hypothesis about the nature of pedestrian flow.

Hypothesis 1. Pedestrians seek to minimize their estimated travel cost based on memory but temper this behavior to avoid high densities.

We further define $\phi(\boldsymbol{x})$ as the minimum travel cost based on the memory from location $\boldsymbol{x} \in \Omega$ to destination Γ_o, at which $\phi(\boldsymbol{x})=0$. We thus write

$$\|\nabla\phi(\boldsymbol{x})\| = c_m(\boldsymbol{x}), \quad \boldsymbol{x} \in \Omega,$$

$$\phi(\boldsymbol{x}) = 0, \quad \boldsymbol{x} \in \Gamma_o, \tag{4}$$

where $c_m(\boldsymbol{x})$ is the perceived local cost per unit distance of movement that was built up in the memory of pedestrians from past experience. This memory effect also reflects the level of familiarity of the pedestrians with the walking facility, which plays an important role in the evacuation process in adverse environmental conditions. Equation (4) is the so-called Eikonal equation.

From hypothesis 1, we have

$$\boldsymbol{f}(\boldsymbol{x},t)//\{-\nabla\phi(\boldsymbol{x}) - \omega\,\nabla\, c(\boldsymbol{x},\rho(\boldsymbol{x},t))\}, \tag{5}$$

where // means that two vectors are parallel and point to the same direction, $-\nabla\phi$ represents the memory effect, ∇c represents the effect of avoiding high densities, and ω is a positive constant that represents the psychological influence. The flow flux direction is implicitly dependent on $\rho(\boldsymbol{x},t)$. When $\omega\to\infty$, the model reduces to the reactive user equilibrium model [26], in which the memory effect vanishes. In contrast, when $\omega\to 0$, pedestrians make route choice decisions based solely on their memory, irrespective of the operating conditions on the walking facility.

In the numerical procedure for the reactive user equilibrium model [26], the Eikonal equation needs to be solved at each time step. With the route choice strategy employed in our model; however, we need only solve the Eikonal equation [Eq. (4)] once at the beginning of the analysis.

B. Well posedness of the linearized equation

There is no general theory for nonlinear differential equations and no global existence theory even if we assume that all of the coefficients and data are smooth functions of the variables. The only general results available are of a local character and can be phrased in the following way. Assume that we know the solution $\bar{\rho}$ for a particular set of data. We then linearize the nonlinear equations around the known so-

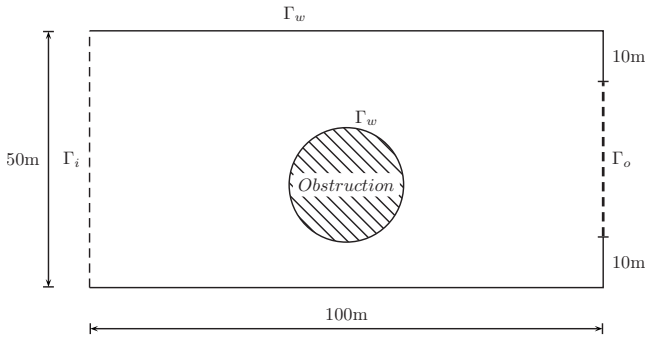

FIG. 1. A railway platform with a circular obstruction. The center of the circle is at (50 m, 20 m) and its area is 400 m^2.

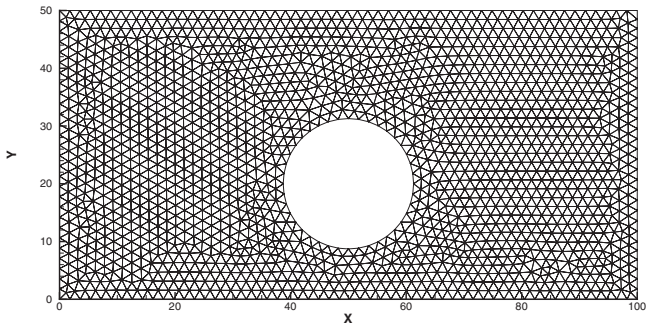

FIG. 2. Triangulations of the platform with circular obstruction.

lution $\bar{\rho}$. The well posedness of the linearized equation is often useful to determine whether the original equations are well posed.

We assume vector $\boldsymbol{n}(\boldsymbol{x},t)=-\nabla\phi(\boldsymbol{x})-\omega\nabla c(\boldsymbol{x},\rho(\boldsymbol{x},t))$, which is parallel to the flow flux $\boldsymbol{f}(\boldsymbol{x},t)$. Equation (1) can be rewritten as

$$\rho(\boldsymbol{x},t)_t+\nabla\cdot(\boldsymbol{f}(\boldsymbol{x},\rho(\boldsymbol{x},t),\nabla\rho(\boldsymbol{x},t)))=0, \tag{6}$$

where $\boldsymbol{f}(\boldsymbol{x},\rho(\boldsymbol{x},t),\nabla\rho(\boldsymbol{x},t))=u(\rho(\boldsymbol{x},t))\rho(\boldsymbol{x},t)\frac{\boldsymbol{n}}{\|\boldsymbol{n}\|}$. The change in variables,

$$\rho(\boldsymbol{x},t)=\bar{\rho}(\boldsymbol{x},t)+\epsilon v(\boldsymbol{x},t),$$

gives the linearized equation

$$v_t+\nabla\cdot[\partial_\rho(\boldsymbol{f}(\boldsymbol{x},\bar{\rho},\nabla\bar{\rho}))v+\partial_{\rho_x}(\boldsymbol{f}(\boldsymbol{x},\bar{\rho},\nabla\bar{\rho}))v_x+\partial_{\rho_y}(\boldsymbol{f}(\boldsymbol{x},\bar{\rho},\nabla\bar{\rho}))v_y]=0, \tag{7}$$

which is a second-order partial differential equation. To show that Eq. (7) is a well-posed problem, we need to check its ellipticity. For simplicity, we assume that the local cost function depends only on the pedestrian density, that is, $c(\rho(\boldsymbol{x},t))$. Thus, we have

$$\partial_{\rho_x}n_2=0,\quad \partial_{\rho_y}n_1=0,\quad \partial_{\rho_x}n_1=\partial_{\rho_y}n_2=-\omega c'(\rho),$$

where $\boldsymbol{n}=(n_1,n_2)$. By substituting this equation into the linearized equation [Eq. (7)], we obtain

$$v_t+\text{first-order terms}+(\partial_{\rho_x}n_1)\frac{|\boldsymbol{f}(\boldsymbol{x},\bar{\rho},\nabla\bar{\rho})|}{\|\boldsymbol{n}\|^3}\times(n_2^2v_{xx}-2n_1n_2v_{xy}+n_1^2v_{yy})=0, \tag{8}$$

which is an elliptic partial differential equation for $c'(\rho)>0$ and is thus well posed.

The stability requirement that $c'(\rho)>0$ is satisfied in most cases. For example, we can choose the pedestrian speed function and cost function employed in [26,27], which are given by

$$U(\rho)=u_{\max}\left(1-\frac{\rho}{\rho_{\max}}\right), \tag{9}$$

$$c(\rho)=\frac{1}{u(\rho)}+\beta g(\rho), \tag{10}$$

where the first term $1/u(\rho)$ represents the local walking time per unit length of movement, $g(\rho)=\rho^2$ in the second term is the discomfort function, $\rho_{\max}$ is the jam density, $u_{\max}$ is the free-flow speed, and β is the coefficient that reflects the sensitivity of pedestrians to the comfort level in their route choice decisions. We now have $c'(\rho)>0$ when $\rho\in(0,\rho_{\max})$, which satisfies the well-posed condition of the linearized equation [Eq. (7)].

We find that the effect of avoiding high densities is the source of the ellipticity in Eq. (7) and that this effect prevents the density from outstripping the jam density, which can be explained as follows. When $\rho\to\rho_{\max}$, we have $c'(\rho)\to+\infty$ and then $\frac{\boldsymbol{n}}{\|\boldsymbol{n}\|}\approx\frac{\nabla\rho}{\|\nabla\rho\|}$. In the peak domain $\Omega_p\in\Omega$, where $\rho\to\rho_{\max}$, $\nabla\rho\cdot\nu\leq 0$, and ν is the outer normal of domain Ω_p, Eq. (1) can be approximated by

$$\rho(\boldsymbol{x},t)_t+\nabla\cdot\left(u(\rho(\boldsymbol{x},t))\rho(\boldsymbol{x},t)\frac{\nabla\rho}{\|\nabla\rho\|}\right)=0,\boldsymbol{x}\in\Omega_p. \tag{11}$$

If we multiply Eq. (11) by density ρ and integrate it over domain Ω_p, then we have

$$\frac{d}{dt}\int_{\Omega_p}\rho^2(\boldsymbol{x},t)d\boldsymbol{x}\leq 0,$$

which verifies that the effect of avoiding high densities prevents the density from outstripping the jam density. This property is also verified in the numerical test presented in Sec. IV.

III. NUMERICAL ALGORITHM

Equation (1), which governs the pedestrian flow, is a scalar two-dimensional conservation law. There have been considerable developments in the algorithms for this type of equation. In [27], we developed a DG method on triangular meshes to solve the reactive dynamic user equilibrium model for pedestrian flows. That model required the Eikonal equation to be solved by the fast sweeping method at each time level. Here, we also adopt the discontinuous Galerkin method developed in [27] to solve the conservation law but

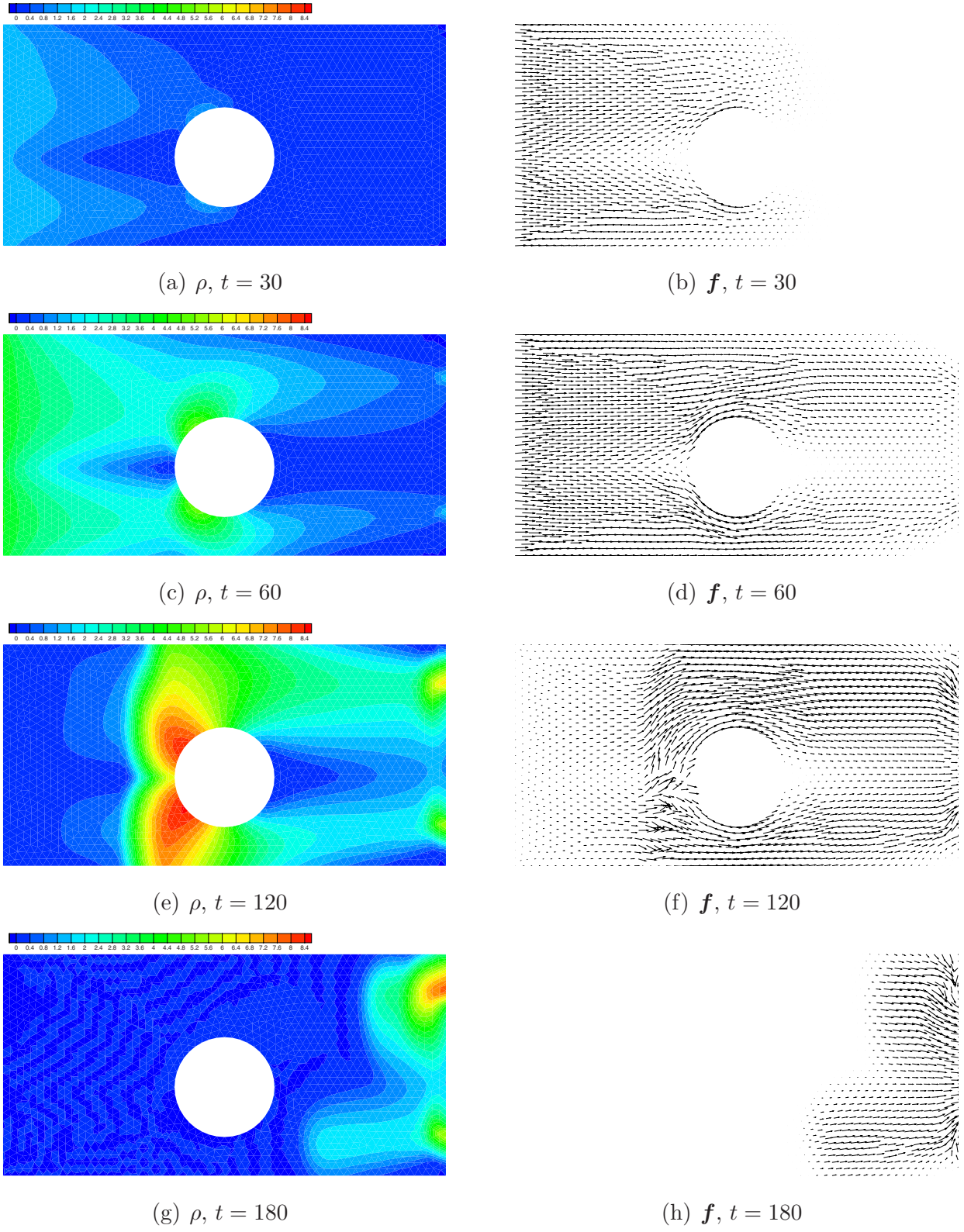

(a) ρ, $t = 30$ (b) $\boldsymbol{f}$, $t = 30$

(c) ρ, $t = 60$ (d) $\boldsymbol{f}$, $t = 60$

(e) ρ, $t = 120$ (f) $\boldsymbol{f}$, $t = 120$

(g) ρ, $t = 180$ (h) $\boldsymbol{f}$, $t = 180$

FIG. 3. (Color online) Density ρ and flux $\boldsymbol{f}$ at different times, t=30, 60, 120, and 180, with ω=1 and β=0.2 on the platform with circular obstruction.

need only solve the Eikonal equation [Eq. (4)] at the beginning of the analysis. We therefore do not address the fast sweeping method on triangular meshes for Eq. (4) here, and instead refer interested readers to [27,43] for details.

We first briefly describe the discontinuous Galerkin method for Eq. (1). Let $\mathcal{T}_h$ denote a tessellation of Ω with shape-regular elements K. Let Γ denote the union of the boundary faces of elements $K \in \mathcal{T}_h$, that is, $\Gamma = \cup_{K \in \mathcal{T}_h} \partial K$ and

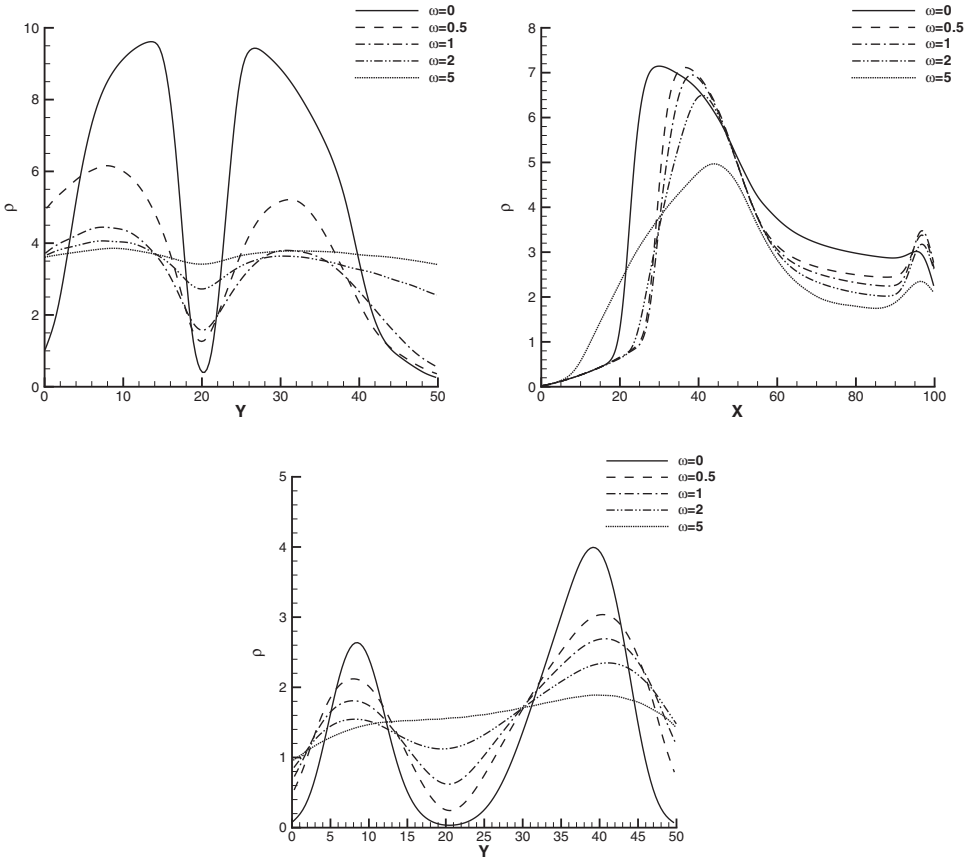

FIG. 4. Density ρ along $x=30$, $y=35$, and $x=80$ at time $t=120$, with $\omega=0$, 0.5, 1.0, 2.0, and 5.0, respectively.

$\Gamma_0=\Gamma\backslash\partial\Omega$. We define the finite element space V_h^k as

$$V_h^k \equiv \{v \in L^2(\Omega): v|_K \in P^k(K), \quad \forall K \in \mathcal{T}_h\}, \tag{12}$$

where $P^k(K)$ denotes the space of the polynomial in K of the degree at most k. Note that the functions in V_h^k are allowed to have discontinuities across the element interfaces.

First, we multiply Eq. (1) by the test function v_h in V_h^k, integrate the result over the element K of triangulation $\mathcal{T}_h$, and replace the exact solution ρ with its approximation, $\rho_h \in V_h^k$, as follows:

$$\frac{d}{dt}\int_K \rho_h(\boldsymbol{x},t)v_h(\boldsymbol{x})d\boldsymbol{x} + \int_K \nabla\cdot\boldsymbol{f}(\boldsymbol{x},t)v_h(\boldsymbol{x})dx = 0, \quad \forall\, v_h \in V_h^k. \tag{13}$$

Integrating by parts, we formally obtain

$$\frac{d}{dt}\int_K \rho_h(\boldsymbol{x},t)v_h(\boldsymbol{x})d\boldsymbol{x} + \sum_{e\in\partial K}\int_e \boldsymbol{f}(\boldsymbol{x},t)\cdot\boldsymbol{n}_{e,K}v_h(\boldsymbol{x})ds - \int_K \boldsymbol{f}(\boldsymbol{x},t)\cdot\nabla v_h(\boldsymbol{x})d\boldsymbol{x} = 0, \quad \forall\, v_h \in V_h^k,$$

where $\boldsymbol{n}_{e,K}$ is the outward unit normal to edge e. Note that $\boldsymbol{f}(\boldsymbol{x},t)\cdot\boldsymbol{n}_{e,K}$ has no precise meaning because ρ_h is discontinuous at $\boldsymbol{x}\in e\in\partial K$. Let $\rho_h^{int(K)}$ denote the value of ρ_h evaluated from inside element K and $\rho_h^{ext(K)}$, the value of ρ_h evaluated from outside element K (inside the neighboring element). We replace $\boldsymbol{f}(\boldsymbol{x},t)\cdot\boldsymbol{n}_{e,K}$ with $h_{e,K}(\rho_h^{int(K)}(\boldsymbol{x},t),\rho_h^{ext(K)}(\boldsymbol{x},t),\boldsymbol{x},t)$, which is any consistent two-point monotone Lipschitz flux that is consistent with $\boldsymbol{f}\cdot\boldsymbol{n}_{e,K}$. Here, we choose the local Lax-Friedrichs flux,

$$h_{e,K}(a,b,\boldsymbol{x},t) = \frac{1}{2}[\boldsymbol{F}(a,\boldsymbol{x},t)\cdot\boldsymbol{n}_{e,K} + \boldsymbol{F}(b,\boldsymbol{x},t)\cdot\boldsymbol{n}_{e,K} - \alpha(b-a)],$$

$$\alpha = \max_{\min(a,b)\le\rho\le\max(a,b)} |U(\rho,\boldsymbol{x},t)|,$$

where $\boldsymbol{F}(\rho,\boldsymbol{x},t) = -U(\rho,\boldsymbol{x},t)\rho(\boldsymbol{x},t)\frac{\boldsymbol{n}}{\|\boldsymbol{n}\|}$. We then replace the integrals according to the following quadrature rules:

$$\int_e \boldsymbol{f}(\boldsymbol{x},t)\cdot\boldsymbol{n}_{e,K}v_h(\boldsymbol{x})ds \approx \sum_{l=1}^{L}\omega_l h_{e,K}(\rho_h^{int(K)}(\boldsymbol{x}_{el},t),\rho_h^{ext(K)} \times(\boldsymbol{x}_{el},t),\boldsymbol{x}_{el},t)v_h(\boldsymbol{x}_{el})|e|,$$

$$\int_K \boldsymbol{f}(\boldsymbol{x},t)\cdot\nabla v_h(\boldsymbol{x},t)dxdy \approx \sum_{j=1}^{M}\kappa_j\boldsymbol{F}(\rho_h(\boldsymbol{x}_{Kj},t),\boldsymbol{x}_{Kj},t)\cdot\nabla v_h(\boldsymbol{x}_{Kj},t)|K|,$$

where $\boldsymbol{x}_{el}$ and ω_l are the quadrature points and weights on edge e, and $\boldsymbol{x}_{Kj}$ and κ_j are those in triangle K. Finally, for

each element $K \in \mathcal{T}_h$, we obtain the following semidiscrete weak formulation:

$$\frac{d}{dt}\int_K \rho_h(\boldsymbol{x},t)v_h(\boldsymbol{x})dxdy + \sum_{e\in\partial K}\sum_{l=1}^{L} \omega_l h_{e,K}(\rho_h^{int(K)}(\boldsymbol{x}_{el},t),\rho_h^{ext(K)} \times(\boldsymbol{x}_{el},t),\boldsymbol{x}_{el},t))v_h(\boldsymbol{x}_{el})|e| - \sum_{j=1}^{M} \kappa_j \boldsymbol{F}(\rho_h(\boldsymbol{x}_{Kj},t),\boldsymbol{x}_{Kj},t)\cdot\nabla v_h(\boldsymbol{x}_{Kj},t)|K| = 0, \quad \forall\, v_h \in V_h^k. \tag{14}$$

The description of the numerical boundary conditions on $\partial\Omega$ is given in the next section.

The semidiscrete Eq. (14) can be rewritten in ordinary differential equation (ODE) form as

$$\frac{d}{dt}\rho_h = L_h(\rho_h), \tag{15}$$

where operator L_h is the spatial DG discrete approximation of $-\nabla\cdot\boldsymbol{f}$. We then use total variation diminishing (TVD) Runge-Kutta methods [33,44] to solve Eq. (15). Starting from density ρ^n at time level t_n, to obtain density ρ^{n+1} at time level t_{n+1} $(:=t_n+\Delta t_n)$, the second-order TVD Runge-Kutta method is given by

$$\rho_h^{(1)} = \rho_h^n + \triangle t_n L_h(\rho_h^n), \tag{16}$$

$$\rho_h^{n+1} = \frac{1}{2}\rho_h^n + \frac{1}{2}\rho_h^{(1)} + \frac{1}{2}\Delta t_n L_h(\rho_h^{(1)}), \tag{17}$$

and the third-order TVD Runge-Kutta method is given by

$$\rho_h^{(1)} = \rho_h^n + \Delta t_n L_h(\rho_h^n), \tag{18}$$

$$\rho_h^{(2)} = \frac{3}{4}\rho_h^n + \frac{1}{4}\rho_h^{(1)} + \frac{1}{4}\Delta t_n L_h(\rho_h^{(1)}), \tag{19}$$

$$\rho_h^{n+1} = \frac{1}{3}\rho_h^n + \frac{2}{3}\rho_h^{(2)} + \frac{2}{3}\Delta t_n L_h(\varphi^{(2)}). \tag{20}$$

The time step $\Delta t_n = \alpha\frac{h}{U_{\max}}$, where h is the minimum of the element diameters in $\mathcal{T}_h$ and $U_{\max}$ is the maximum pedestrian walking speed. The constant α is dependent on the degree of the polynomial in the DG method and on the order of the Runge-Kutta method [38].

IV. NUMERICAL TESTS

Consider a railway platform with a circular obstruction in the middle, as shown in Fig. 1. Pedestrians enter this platform from the left boundary Γ_i and leave from the right boundary Γ_o. The platform is initially empty $[\rho(\boldsymbol{x},0)=0]$, and the boundary conditions on Γ_i are

$$\boldsymbol{f} = \begin{cases} (t/12,0), & 0 \le t \le 60 \\ (10-t/12,0), & 60 \le t \le 120 \\ (0,0), & t \ge 120. \end{cases}$$

There is an outflow boundary condition on Γ_o, and the solid-wall boundary condition on Γ_w is $\boldsymbol{f}(\boldsymbol{x},t)=0$. The pedestrian speed and the cost function are given by Eqs. (9) and (10), respectively, with $u_{\max}=2$ and $\rho_{\max}=10$. In this example, we assume that $c_m(\boldsymbol{x})$ is the local cost when there are no pedestrians (i.e., $\rho=0$). In other words, $c_m=1/u_{\max}$ is a constant.

In practice, we often solve nonlinear problems numerically with no knowledge of whether the differential equations have any solution. If the numerical solution varies slowly with respect to the mesh or the approximation space, then the original problem can be viewed as a perturbation of that numerical solution. In the example employed here, we use the third-order DG method coupled with the second-order fast sweeping method and the third-order TVD Runge-Kutta method. As can be seen in Fig. 2, there are 3417 elements in the triangulations of the platform with circular obstruction. We initially use the fast sweeping method described in [27] to solve the Eikonal equation [Eq. (4)] and to obtain the memory information ϕ and $\nabla\phi$. We then use the numerical algorithm described in Sec. III to evolve the governing equation [Eq. (1)]. We also perform simulations using the first- and second-order polynomial basis of the DG method, but the numerical results are comparable to those of the third-order DG method.

In Fig. 3, we plot the density ρ and flux $\boldsymbol{f}$ with $\omega=1$, $\beta=0.2$ at times $t=30$, 60, 120, and 180, respectively, to show the movement pattern of pedestrians who walk around the obstruction in the middle of the platform and head toward the exit. The density increases steadily and reaches its maximum near time $t=120$. As the time nears $t=240$, the density returns to zero. Around $t=120$ [see Fig. 3(e)], two shocks can clearly be seen in front of the obstruction due to the reduction in the width of the corridor. Such shocks are frequently observed in walking facilities when large crowds of pedestrians queue up to walk through a bottleneck with reduced capacity. Triangular vacuum regions are also observed in front of [Fig. 3(c)] and behind the obstruction [Fig. 3(e)], which is consistent with the route choice strategy. These phenomena can also be observed in the reactive equilibrium pedestrian model [26,27]. The shocks in the model with memory are stronger than those in the reactive equilibrium model because of the memory effect, whereby pedestrians are attracted to the optimal route based on their memory despite it being congested. The vacuum regions in the former model are also smaller than those in the latter for the same reason.

To further illustrate the route choice strategy, in Figs. 4 and 5 we plot the density ρ and flux $\boldsymbol{f}$ along $x=30$, $y=35$, and $x=80$ at time $t=120$ with $\omega=0$, 0.5, 1.0, 2.0, 5.0, and $\beta=0.2$, respectively. In our linearized analysis, the effect of avoiding high densities is the source of the ellipticity in the linearized equation. When psychological influence parameter ω increases, both the density and the flux become smooth, which further demonstrates that the memory effect produces stronger shocks.

In Fig. 6, we give the total travel time $\int\int_\Omega \rho(\boldsymbol{x},t)d\boldsymbol{x}dt$ with different ω and β. When β is fixed, the total travel time is a convex function of ω. When ω increases, the total travel time first decreases and then increases, which demonstrates the importance of the memory effect during an evacuation. When the environmental conditions are significantly degraded, the evacuation process depends solely on the

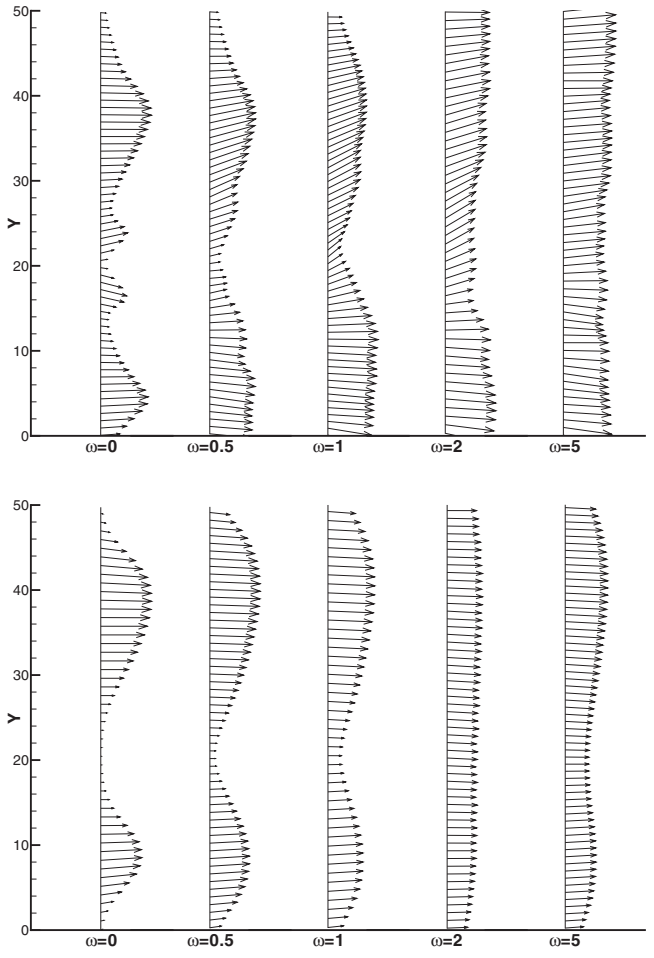

FIG. 5. Flux $\boldsymbol{f}$ along $x=30$ and $x=80$ at time $t=120$, with $\omega=0$, 0.5, 1.0, 2.0, and 5.0, respectively.

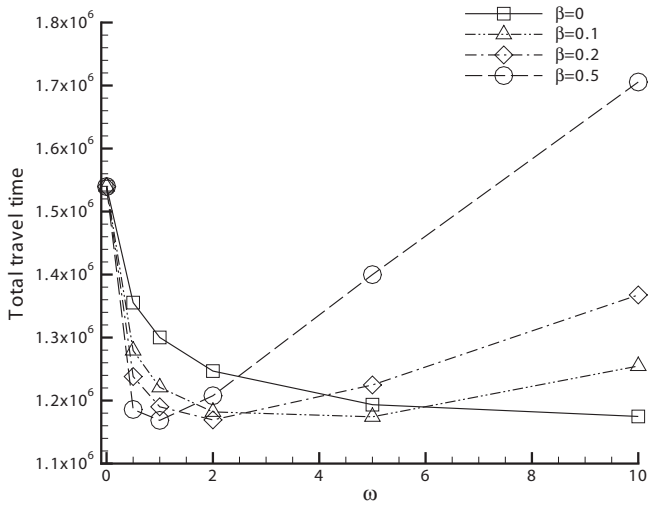

FIG. 6. Total travel time $\int\int \rho(\boldsymbol{x},t)d\boldsymbol{x}dt$, with $\omega=0$, 0.5, 1.0, 2.0, 5.0, and 10 and $\beta=0$, 0.1, 0.2, and 0.5, respectively.

memory of the pedestrians, which increases the total evacuation time because pedestrians are attracted to the optimal routes in their memory and fail to avoid crowds. This is particularly problematic for evacuation in severe environments, such as smoky conditions during escape from a fire or a dark room with insufficient lighting. However, for a crowd that is unfamiliar with the environment of the walking facility, in which the memory effect is very low (i.e., with a large ω), the evacuation time is also increased. Therefore, proper training and education to improve familiarization with evacuation instructions are essential for pedestrian evacuation. This is particularly important for inexperienced pedestrians who are unable to identify the quickest route and tend to reactively switch to less crowded regions during evacuation (i.e., with a large β).

V. CONCLUSION

In this study, we develop a dynamic continuum model for pedestrian flow in which the route choice strategy is based on the hypothesis that pedestrians seek to minimize their perceived travel cost based on memory but temper this behavior to avoid high densities. The main advantages of the model are that it does not require that pedestrians anticipate changes in the operating conditions over time, especially when they are not familiar with the likely responses of a crowd, and allows for circumstances in which the quality of the instantaneous information available may be degraded due to adverse environmental conditions such as bad weather, insufficient lighting, and smoky conditions. We provide an analytical study to describe the well posedness of the problem, which demonstrates the existence of a solution and the mathematical validity of the developed model.

The discontinuous Galerkin method is employed to solve the model. In contrast to that in [20,26], the present method does not require the Eikonal equation to be solved numerically at each time step, which is the most time-consuming aspect of the numerical procedure [27]. A numerical test is performed to demonstrate both the model and the effectiveness of the numerical method. The results demonstrate the important role of the memory effect in the pedestrian evacuation process. This model will serve as a useful tool in the planning and design of walking facilities.

In this paper, we consider only a single commodity of pedestrian flow. A multicommodity pedestrian model will be developed in a future research. The model presented in this paper can be viewed as falling between the predictive and reactive models. It would be interesting to construct a systematic framework that explains all of these route choice strategies.

ACKNOWLEDGMENTS

The work described in this paper was supported by a grant from the Research Grants Council of the Hong Kong Special Administrative Region of China (Project No. HKU 7183/06E), by ARO (Grant No. W911NF-08-1-0520), and NSF (Grant No. DMS-0809086).

[1] D. Helbing, Rev. Mod. Phys. **73**, 1067 (2001).
[2] A. Schadschneider, W. Klingsch, H. Klupfel, T. Kretz, C. Rogsch, and A. Seyfried, in *Complex Dynamics of Traffic Management*, edited by B. Kerner, Encyclopedia of Complexity and System Science (Springer, New York, 2009), Article No. 00754.
[3] V. J. Blue and J. L. Adler, Transp. Res., Part B: Methodol. **35**, 293 (2001).
[4] C. Burstedde, K. Klauck, A. Schadschneider, and J. Zittartz, Physica A **295**, 507 (2001).
[5] A. Kirchner and A. Schadschneider, Physica A **312**, 260 (2002).
[6] W. G. Weng, T. Chen, H. Y. Yuan, and W. C. Fan, Phys. Rev. E **74**, 036102 (2006).
[7] D. Helbing and P. Molnar, Phys. Rev. E **51**, 4282 (1995).
[8] D. Helbing, I. J. Farkas, and T. Vicsek, Nature (London) **407**, 487 (2000).
[9] D. R. Parisi and C. O. Dorso, Physica A **354**, 606 (2005).
[10] T. I. Lakoba, D. J. Kaup, and N. M. Finkelstein, Simulation **81**, 339 (2005).
[11] M. Muramatsu, T. Irie, and T. Nagatani, Physica A **267**, 487 (1999).
[12] M. Muramatsu and T. Nagatani, Physica A **286**, 377 (2000).
[13] D. Helbing, M. Isobe, T. Nagatani and K. Takimoto, Phys. Rev. E **67**, 067101 (2003).
[14] R. Y. Guo and H. J. Huang, Physica A **387**, 580 (2008).
[15] G. D. Gaskell and R. J. Benewick, *The Crowd in Contemporary Britian* (Sage, London, 1987).
[16] S. C. Wong, Transp. Res., Part B: Methodol. **32**, 567 (1998).
[17] S. C. Wong, C. K. Lee, and C. O. Tong, Int. J. Numer. Methods Eng. **43**, 1253 (1998).
[18] H. W. Ho, S. C. Wong, and B. P. Y. Loo, Transp. Res., Part B: Methodol. **40**, 633 (2006).
[19] H. W. Ho and S. C. Wong, Transportmetrica **3**, 21 (2007).
[20] R. L. Hughes, Transp. Res., Part B: Methodol. **36**, 507 (2002).
[21] S. P. Hoogendoorn, P. H. L. Bovy, and W. Daamen, J. Adv. Transp. **38**, 69 (2003).
[22] S. P. Hoogendoorn and P. H. L. Bovy, Transp. Res., Part B: Methodol. **38**, 169 (2004).
[23] S. P. Hoogendoorn and P. H. L. Bovy, Transp. Res., Part B: Methodol. **38**, 571 (2004).
[24] M. Asano, A. Sumalee, M. Kuwahara, and S. Tanaka, Transp. Res. Rec. **2039**, 42 (2007).
[25] C. O. Tong and S. C. Wong, Transp. Res., Part B: Methodol. **34**, 625 (2000).
[26] L. Huang, S. C. Wong, M. Zhang, C.-W. Shu, and W. H. K. Lam, Transp. Res., Part B: Methodol. **43**, 127 (2009).
[27] Y. Xia, S. C. Wong, M. P. Zhang, C.-W. Shu, and W. H. K. Lam, Int. J. Numer. Methods Eng. **76**, 337 (2008).
[28] W. H. Reed and T. R. Hill, Los Alamos Scientific Laboratory, Los Alamos, NM Technical Report No. LA-UR-73-479, 1973 (unpublished).
[29] B. Cockburn and C.-W. Shu, Math. Comput. **52**, 411 (1989).
[30] B. Cockburn, S.-Y. Lin, and C.-W. Shu, J. Comput. Phys. **84**, 90 (1989).
[31] B. Cockburn, S. Hou, and C.-W. Shu, Math. Comput. **54**, 545 (1990).
[32] B. Cockburn and C.-W. Shu, J. Comput. Phys. **141**, 199 (1998).
[33] C.-W. Shu and S. Osher, J. Comput. Phys. **77**, 439 (1988).
[34] K. S. Bey, A. Patra, and J. T. Oden, Int. J. Numer. Methods Eng. **38**, 3889 (1995).
[35] K. S. Bey and J. T. Oden, Comput. Methods Appl. Mech. Eng. **133**, 259 (1996).
[36] B. Cockburn, *High-Order Methods for Computational Physics*, Lecture Notes in Computational Science and Engineering Vol. 9, edited by T. J. Barth and H. Deconinck (Springer, New York, 1999) pp. 69–224.
[37] B. Cockburn, G. Karniadakis, and C.-W. Shu, *Discontinuous Galerkin Methods: Theory, Computation and Applications*, Lecture Notes in Computational Science and Engineering Vol. 11, edited by B. Cockburn, G. Karniadakis, and C.-W. Shu (Springer, New York, 2000), pp. 3–50.
[38] B. Cockburn and C.-W. Shu, J. Sci. Comput. **16**, 173 (2001).
[39] J. Palaniappan, R. B. Haber, and R. L. Jerrard, Comput. Methods Appl. Mech. Eng. **193**, 3607 (2004).
[40] J. F. Remacle, X. R. Li, M. S. Shephard, and J. E. Flaherty, Int. J. Numer. Methods Eng. **62**, 899 (2005).
[41] F. Shakib, T. J. R. Hughes, and Z. Johan, Comput. Methods Appl. Mech. Eng. **89**, 141 (1991).
[42] A. Smolianski, O. Shipilova, and H. Haario, Int. J. Numer. Methods Eng. **70**, 655 (2007).
[43] J. Qian, Y.-T. Zhang, and H.-K. Zhao, SIAM (Soc. Ind. Appl. Math.) J. Numer. Anal. **45**, 83 (2007).
[44] S. Gottlieb and C.-W. Shu, Math. Comput. **67**, 73 (1998).